Journal of Earth Science, *Vol. 31*, *No. 2*, *p. 410–418*, *April 2020* *ISSN 1674-487X*
Printed in China
https://doi.org/10.1007/s12583-019-1238-5

Potential Effect of Black Carbon on Glacier Mass Balance during the Past 55 Years of Laohugou Glacier No. 12, Western Qilian Mountains

Jizu Chen[1], **Xiang Qin**[1], **Shichang Kang**[1, 2], **Wentao Du***[1], **Weijun Sun**[3], **Yushuo Liu**[1]
1. *Qilian Shan Station of Glaciology and Ecological Environment*, *State Key Laboratory of Cryospheric Sciences*, *Northwest Institute of Eco-Environment and Resources*, *Chinese Academy of Sciences* (*CAS*), *Lanzhou* 730000, *China*
2. *CAS Center for Excellence in Tibetan Plateau Earth Sciences*, *Beijing* 100085, *China*
3. *College of Geography and Environment*, *Shandong Normal University*, *Jinan* 250014, *China*
Jizu Chen: https://orcid.org/0000-0002-3066-0726; Wentao Du: https://orcid.org/0000-0002-5522-148X

ABSTRACT: This study reconstructed the annual mass balance (MB) of Laohugou Glacier No. 12 in the western Qilian Mountains during 1961–2015. The annual MB was calculated based on a temperature-index and an accumulation model with inputs of daily air temperature and precipitation recorded by surrounding meteorological stations. The model was calibrated by *in-situ* MB measurements conducted on the glacier during 2010–2015. Change in constructed annual MB had three phases. During Phase I (1961–1984), glacier-wide MB values were slightly positive with an average MB of 24±276 mm w.e. (water equivalent). During Phase II (1984–1995), the MB values became slightly negative with an average MB of -50±276 mm w.e.. The most negative MB values were found during Phase III (1996–2015), with an average MB of -377±276 mm w.e. Climatic analysis showed that the warming led to accelerated glacier mass loss despite a persistent increase of precipitation during the analysis period. However, an increase of black carbon deposited on the glacier surface since the 1980s could have contributed to intensified glacier melt. From simulations and measurements of MB on the Urumqi Glacier No. 1, 26% of glacier melt caused by black carbon could be identified.
KEY WORDS: Laohugou Glacier No. 12, climate change, temperature-index model, mass balance, black carbon.

0 INTRODUCTION

The Tibetan Plateau (TP) and surrounding areas contain the largest number of glaciers outside the polar regions (Yao et al., 2012). Those glaciers contribute to water supply of millions of people (Lutz et al., 2014; Immerzeel et al., 2010). In the context of global warming, glaciers on the TP are experiencing widespread shrinkage (Yao et al., 2012; Kang et al., 2010); however, the pattern of glacier change on the TP and in surrounding areas is now known to be strongly heterogeneous. For instance, more than 65% of the monsoon-influenced glaciers in the Himalayan region are retreating, whereas those with heavy debris cover and stagnant low-gradient terminus regions typically have stable fronts (Scherler et al., 2011). Different from the general background, an anomalous slightly positive glacier mass budget in the Karakoram has been documented, attributable to increased winter precipitation in this region (Gardelle et al., 2013, 2012). Experiential glacial melt models such as a physically based Holmgren, 2005; Fujita and Ageta, 2000) and a temperature energy and mass balance model (Mölg et al., 2009; Hock and Holmgren, 2005; Fujita and Ageta, 2000) and a temperature-index model (Huss et al., 2008; Hock, 2003) could be used to link atmospheric variables with glacier melt. Many previous studies have focused on large-scale glacier mass balance (MB) recovery and prediction (Kraaijenbrink et al., 2017; Lutz et al., 2014; Marzeion et al., 2014; Immerzeel et al., 2010). However, limited by a lack of glaciological measurements, the parameters have always been calibrated using only a few local measurements. For instance, MB measurements and parameters are only available based on data from the Qiyi Glacier in the Qilian Mountains. Over the entire TP long-term series of MB measurements are available only from 15 glaciers (Yao et al., 2012). Therefore, surveying of glacier MB, especially over the long term, remains vitally important in relation to glacier melt modeling.

Light-absorbing particles (LAPs) such as black carbon (BC) have become secondary source of global warming (IPCC, 2013). BC can absorb solar radiation and accelerate glacier melt when settling on the snow and ice surface (Li et al., 2016; Xu et al., 2009; Bond et al., 2004). Kopacz et al. (2011) estimated radiative forcing of 5–15 W m^{-2} attributable to BC within snow-covered areas of the Himalaya and the TP. Flanner et al. (2007) and Qian et al. (2011) estimated peak values of the effect of BC exceeded 20 W·m^{-2} in some parts of the TP. Such a change in radiation could greatly influence the process of the glacial

*Corresponding author: duwentao@lzb.ac.cn

Manuscript received March 1, 2019.
Manuscript accepted September 5, 2019.

Chen, J. Z., Qin, X., Kang, S. C., et al., 2020. Potential Effect of Black Carbon on Glacier Mass Balance during the Past 55 Years of Laohugou Glacier No. 12, Western Qilian Mountains. *Journal of Earth Science*, 31(2): 410–418. https://doi.org/10.1007/s12583-019-1238-5. http://en.earth-science.net

energy balance (Sun et al., 2014, 2012).

The Qilian Mountains located at the northeastern fringe of the TP act as the water source for the Hexi Corridor in China. The Qilian Mountains contain 2 693 glaciers which occupy a total area of about 1 598 km^2 (Guo et al., 2015, the second Chinese glacier inventory). However, over the past century, glaciers in the Qilian Mountains have experienced rapid thinning and shrinkage. In the western Qilian Mountains, the areas and volumes of glaciers have decreased by 15% and 18%, respectively, from the Little Ice Age maximum to 1956 (Liu et al., 2003). Alarmingly, during 1956–2010, the glacier area in the entire region of the Qilian Mountains has decreased by 30%±8% (Tian et al., 2014). Kraaijenbrink et al. (2017) demonstrated that under global warming of 1.5 °C, the glacier area in the Qilian Mountains could be reduced to only 32% of current area by the end of the century, representing the greatest potential glacial loss on the TP.

This study presented 55 years' MB variability of the Laohugou Glacier No. 12 (LHG Glacier) in the western Qilian Mountains, China. The aims of the investigation are (i) to summarize glacier fluctuations over the past 55 years, (ii) to elucidate quantitatively the relationship between climate change and glacier fluctuation, (iii) and to highlight the potential effect of increased BC deposition since the 1980s on glacial melt and glacial modeling.

1 STUDY SITE

The LHG Glacier (39°26.4′N, 96°32.5′E), a valley-type nonsurging one, is located in the upstream region of the Shulehe River basin in the western Qilian Mountains (Fig. 1). The glacier descends from an elevation of 5 480 to 4 260 m a.s.l.. It has overall length of 9.7 km and covers an area of 20.37 km^2 (Liu et al., 2018), the largest valley-type glacier in the Qilian Mountains. The glacier has two branches that converge at the elevation of 4 550 m a.s.l.. Northern Hemisphere mid-latitude westerlies dominate the climate of this region throughout the year.

During recent decades, the LHG Glacier has experienced severe mass loss and shrinkage. During 1960–2015, the glacier length decreased by 403 m (3.99% of its total length) and the glacier area decreased by 1.54 km^2 (7.03% of its total area) (Liu et al., 2018). The equilibrium-line altitude ascended from the average of 4 800 m a.s.l. during the 1970s to 5 015 m a.s.l. during 2010–2012 (Chen et al., 2017).

2 DATA

Research on the LHG Glacier began in 1958 and the nearby glacier station was one of the earliest adopted for glaciology research in China. During 1958–1962, researchers monitored local meteorology and hydrology, and performed glacier mapping and MB, and ice temperature surveys. Unfortunately, the station was closed in 1962 because of a glacial flood. Only in the 1970s–1980s were some short-term observations performed in relation to studies on glacier change and its influence on the water resource. The Qilian Shan Station of Glaciology and Ecologic Environment was rebuilt in 2005 to focus on research in the fields of glaciology (Chen et al., 2018; Sun et al., 2014, 2012), ecology, and the atmospheric environment (Dong et al., 2019, 2018a, b) of this remote area. This study used measurements of the glacier and the atmosphere to run the melt model.

2.1 Mass Balance Data

During 1976, the ground stereo photogrammetry and mass balance measurements were carried out by previous glaciologists (Sun and Xie, 1981), the glacier-wide mass balance was 330 mm w.e. during the year.

Since 2010, *in-situ* MB measurements on the LHG Glacier have been determined on a monthly basis during May–September. Approximately 40 plastic stakes have been drilled into the ice to measure glacier ablation (Fig. 1). In the accumulation zone, snow pits were dug to measure the depth and density of the snow. Measured ice ablation was converted into water equivalent assuming an ice density of 900 kg·m^{-3}.

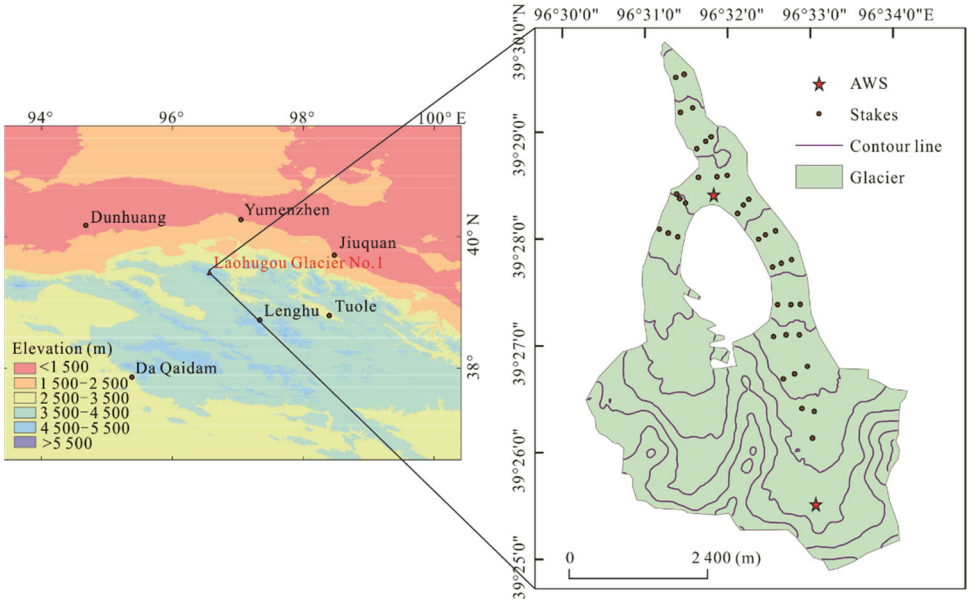

Figure 1. Maps showing location of the Laohugou Glacier No. 12 and the surrounding national meteorological stations.

2.2 Meteorological Data

Meteorological data from the LHG Glacier have been available since 2009 from an automatic weather station (AWS). The station is located at the elevation of 4 200 m a.s.l., 1.6 km from the terminus of the LHG Glacier (Fig. 1). Half-hourly air temperature (T) was measured using a Vaisala 41382 sensor (Campbell Scientific Inc.). Precipitation (P) was measured using an all-weather precipitation gauge (Geonor T-200B) without heating. The sensors were connected to a low-temperature resistant (-55 °C) data logger (CR1000, Campbell Scientific Inc., USA). Detailed descriptions of instruments can be found in Sun et al. (2014). Figure 2 shows the monthly average air temperature and accumulated precipitation at the AWS during 2009–2015. The average air temperature was -5.9 °C and the yearly total amount of precipitation was 344 mm w.e. (water equivalent).

2.2.1 Air temperature

To derive T since 1960, data were collected from six adjacent weather stations (Fig. 1) within a horizontal distance of 250 km from the LHG Glacier. The data were observed by the national meteorological observation network of the China Meteorological Administration (Table 1). Stations of Dunhuang, Yumenzhen, and Jiuquan lie on the northern slopes of the Qilian Mountains, the Tuole is in the alpine area, and the Da Qaidam and Lenghu are located on the southern slopes. These stations were established in the 1950s and records of daily T were available. Strict quality control was applied by the National Meteorological Information Center (Wang, 2004).

Data from the six stations were interpolated to the site of the LHG Glacier AWS. Having compared several interpolation techniques, (e.g., the inverse distance weighted, spline, and ordinary kriging methods and the multiple regression equation), Du et al. (2011) found the ordinary kriging method had the best performance compared with observed T at the AWS. We reconstructed T at the AWS using the ordinary kriging interpolation method, as suggested by Du et al. (2011). The R^2 was 0.995 and the root mean square error (RMSE) was 0.51 between the reconstructed monthly T and that measured by the AWS during 2009–2015 (p<0.001, n=72).

2.2.2 Precipitation

The westerlies dominate the climate of the middle and western Qilian Mountains, whereas the climate of the eastern Qilian Mountains is dominated by both the westerlies and southeastern monsoon (Morrill et al., 2003). We compared precipitation between the LHG Glacier and the surrounding national stations and found the best match with Tuole. Figure 3 shows the amount of annual P during 1961–2015 at Tuole.

3 METHODS

The monthly MB was calculated using a simple temperature-index model together with an accumulation model. The temperature-index model relates glacier melt with the PDD via a constant of proportionality called the degree-day factor (DDF, mm·d^{-1}·°C^{-1}), which is used widely in glaciology for its high computational efficiency. Ablation M can be given by

$$M = \mathrm{DDF}_{s,i} \sum \mathrm{PDD} \tag{1}$$

PDD is calculated by assuming that air temperature follows law of normal distribution, and monthly average air temperature is given as harmonic wave of air temperature

$$T_d(t) = T_a + T_1 \cos\left(\frac{2\pi t}{A}\right) + T_2 \sin\left(\frac{2\pi t}{A}\right) \tag{2}$$

where A is the sum of days; T_a is the annual average temperature; T_1 and T_2 are regression parameters. PDD can be given by

$$\mathrm{PDD}_{th} = \int_{A_1}^{A_2} \frac{1}{\delta\sqrt{2\pi}} \int_0^{\infty} e \frac{(T_d(t) - T_m)^2}{2\delta^2} dT dt \tag{3}$$

where δ is the standard deviation of air temperature; T_m is the average temperature during a month; A_1 and A_2 are days of start and end.

Table 1 List of the names and the latitude, longitude, elevation, and observation periods of stations used in this study

Station name	Latitude (N)	Longitude (E)	Elevation (m a.s.l.)
Dunhuang	40°09′	94°41′	1 139
Yumenzhen	40°16′	97°02′	1 526
Jiuquan	39°46′	98°29′	1 477
Tuole	38°48′	98°25′	3 367
Da Qaidam	37°51′	95°22′	2 982
Lenghu	38°44′	97°20′	2 766

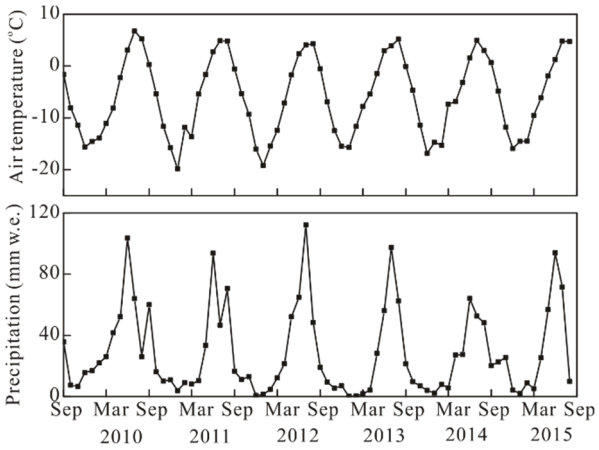

Figure 2. Monthly average air temperature and accumulated precipitation at site of AWS during 2009–2015.

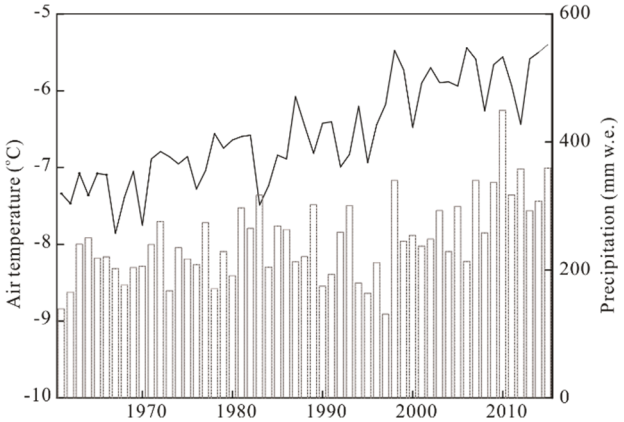

Figure 3. Annual average air temperature (black line) and sum of precipitation (gray bars) at the Tuole station during 1961–2015.

Snow accumulation A (mm w.e.) was calculated based on measured daily *P*. The *P* was divided into snow, rain, and a mixture of the two according to daily *T*. The occurrence of snow and rain was determined based on the threshold temperature of 0 and 2 °C, respectively. A mixture of rain and snow was assumed at *T* between 0 and 2 °C. Within this range of *T*, the snow percentage of total *P* was obtained by linear interpolation (Hock and Holmgren, 2005).

The MB was calculated at a 50-m-elevation interval. The glacier-wide MB was estimated as the sum of the MB during one year multiplied by the area ratio of each elevation band. The *T* and *P* at each elevation band were computed according to a lapse rate of -0.6 °C· (100 m)$^{-1}$ and precipitation gradient of +9%· (100 m)$^{-1}$ (Chen et al., 2017), respectively. In the upper of belt of superimposed ice, we assumed 10% of snow melt to percolate into deep snow and freeze into ice.

4 RESULTS

4.1 Model Calibration and Validation

On the LHG Glacier, the DDFs for the ice and snow parts were obtained based on linear regression between point ablation measurements and the corresponding PDD. The point ablation measurements were performed during the summers of 2010–2012 at elevations in the range 4 300–5 000 m a.s.l.. On the LHG Glacier, the average DDF for ice was 7.5 mm·d^{-1}·°C^{-1}, ranging from 5.5 to 9.9 mm·d^{-1}·°C^{-1}. The DDF for snow fluctuated between 2.1 and 5.4 mm·d^{-1}·°C^{-1}, with an average value of 3.4 mm·d^{-1}·°C^{-1} (Fig. 4). The increase of DDF with elevation showed a low-temperature effect, which resulted from more intense solar radiation at higher elevations (Xu et al., 2017; Kayastha, 2003). The variation of DDF on the LHG Glacier was found consistent with that of both the Qiyi Glacier (Kayastha et al., 2003) and the Urumqi Glacier No. 1 (Cui et al., 2013). Zhang et al. (2006) reported the mean value of DDF for ice in western China on the monitored glaciers was 7.1 mm·d^{-1}·°C^{-1}, whereas it was 4.1 mm·d^{-1}·°C^{-1} for snow. Maritime glaciers were found likely to have higher DDF values than subcontinental and continental glaciers did.

The MBs were simulated using DDF values of 7.5 mm·d^{-1}·°C^{-1} for ice and 3.4 mm·d^{-1}·°C^{-1} for snow, respectively, and the results were validated based on the measured MB gradient with elevation for each hydrological year between 2009 and 2015 (Fig. 5, note the MB of 2012/2013 was not included). The modeled MBs had reasonable agreement with the measurements as indicated by a general RMSE of 276 mm·w.e.a^{-1}. The best agreement was found in 2010/2011 (RMSE: 183 mm·w.e.a^{-1}) and the worst agreement was found in 2013/2014 (RMSE: 462 mm·w.e.a^{-1}). The largest discrepancies were found in the ablation zone below 4 600 m a.s.l.. This was because the glacier is steeper and narrower in the ablation zone and the debris thickness is inhomogeneous. Thus, the MBs varied widely between different sites and different years.

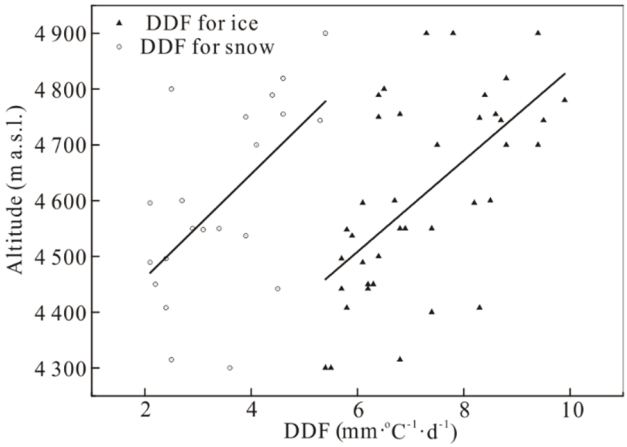

Figure 4. DDF distribution for snow and ice with elevation. Black lines show linear regression between elevation and DDF.

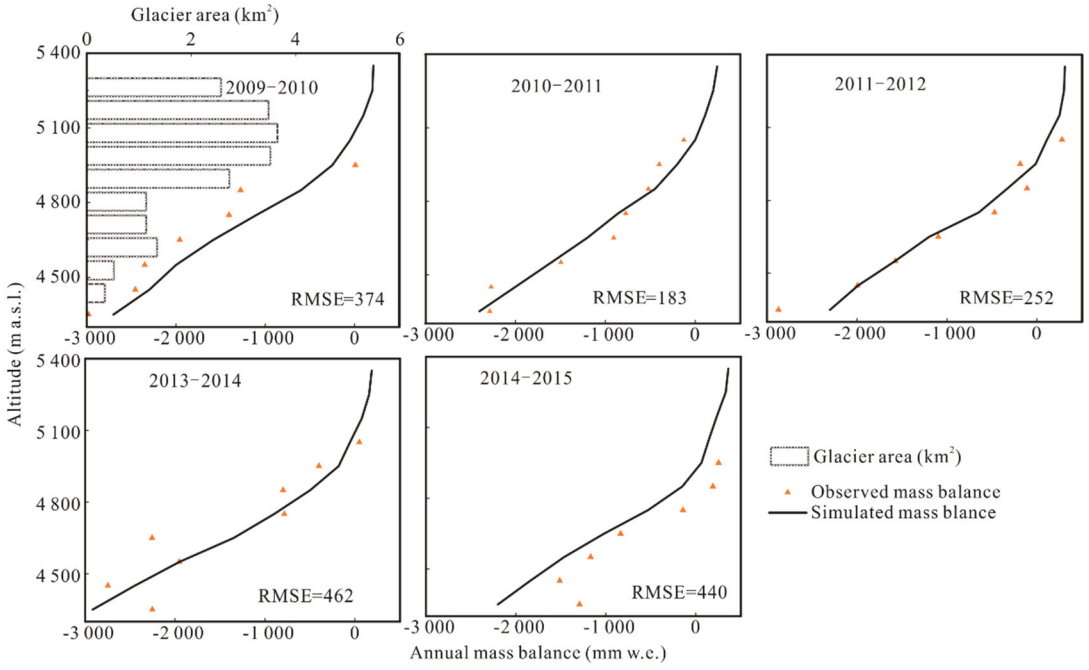

Figure 5. Observed and simulated mean annual mass balance profiles, and glacier area distribution with specific elevation bands of Laohugou Glacier No. 12. RMSE (mm·w.e.a^{-1}) for each year is also given.

4.2 Annual Glacier-Wide Mass Balance since 1961

We reconstructed the MB of the LHG Glacier since 1960 based on measured daily *T* and *P*, and the glacier-wide MBs were displayed in Fig. 6. The reconstructed annual MBs had a good agreement with the measured values, the reconstructed and measured average glacier-wide MB were -165 and 150 mm w.e., respectively, the RMSE was 36.4 mm w.e. between them. The relative span of annual MB between the year with the weakest melt in 1975 (300 mm w.e.) and the year with the most intense melt in 2006 (-620 mm w.e.) was about 920 mm w.e., where the average value was -126.79±35 mm w.e. during 1960–2015.

Three periods with different melting rates could be roughly identified: 1960–1983 (Period I), 1984–1995 (Period II), and 1996–2015 (Period III). These were found accordant with both the Urumqi Glacier No. 1 (Li et al., 2011) and the Qiyi Glacier (Wang et al., 2010). During Period I, the glacier-wide MB was found slightly positive (24±276 mm w.e.). During Period II, the MB became slightly negative (-50±276 mm w.e.). The most negative MB of -377±276 mm w.e. was found during Period III.

Compared to other glaciers in the TP and surroundings, the LHG Glacier showed relative weak melting during past decades. Che et al. (2017) reviewed measurements of MB carried out on TP glaciers, and found that the average MB was -260 mm w.e. per year during 1959–2015. Azam et al. (2014) reconstructed MB of the Chhota Shigri Glacier by a temperature-index model since 1969. The MB in this glacier was -300 mm w.e.a^{-1} over the period of 1969–2012 (Azam et al., 2014). Observations showed that the MB on the Urumqi Glacier No. 1 was -287 mm w.e.a^{-1} during 1960–2008 (Li et al., 2011). On the Qiyi Glacier middle of Qilian Mountains, the MB was -272 mm·w.e.a^{-1} during 1957–2013 (Wang et al., 2015).

Azam et al. (2014) reported accelerated glacier mass loss during the past five decades on the Chhota Shigri Glacier in the western Himalayan region, despite the MB during Period II being much less negative than Period I and near to balance, which was different from the glaciers of the northern TP. The anomaly resulted from *P* and *T* that were 56 mm·a^{-1} higher and 0.2 °C lower than the summer mean, respectively, in comparison with the 1969–2012 averages. *P* did not increase significantly, whereas *T* increased continuously on the glaciers of the northern TP during the period. This could be attributed to the different climatic regimes; the south of the TP is under the dominance of the Indian monsoon and westerlies, while the northern TP is mainly under the influence of westerlies (Maussion et al., 2014; Yao et al., 2012).

5 DISCUSSION

5.1 Response of Glacier Mass Balance to Climate Change

During the past six decades, *T* has increased continuously (Fig. 3), from -7.3 °C during 1961–1970 to -5.8 °C during 2001–2015. The LHG Glacier has experienced dramatic mass loss despite the gradual increase of *P*. The MB change was found to correlate well with the variations of *T* (*R*=0.78). To discuss the response of glacier MB to climate change, we divided the 55 years of the study period into six periods according to 10-year intervals. The MB was near to balance during 1961–1970, thus we took this period as the background reference period. Figure 7 shows the decadal variations of *T*, *P*, and MB relative to 1961–1970. Before 2000, *T* increased gently at the rate of 0.3 °C·(10a)$^{-1}$. Then, during 2000–2010, it increased sharply at the rate of 0.6 °C· (10a)$^{-1}$. Because of the function of *P*, the glacier did not experience consistent aggravated mass loss. During 1971–1980, *T* increased by 0.4 °C, while *P* increased by 19 mm w.e. (9%); thus, the MB increased positively by 35 mm w.e.. During 1981–1990, the negative increase of MB, attributable to the 0.6 °C increase of *T*, was approximately offset by the 50 mm w.e. (25%) increase of *P*. In subsequent years, the negative increase of MB was substantial despite the increase of *P*. During 2000–2010, *T* increased by 1.5 °C and *P* increased by 88 mm w.e. (44%). Consequently, the MB increased negatively by -425 mm w.e.. After 2010, the increase of *T* remained at 1.5 °C, while *P* increased by 125 mm w.e. (0.62); thus, the MB increased negatively by -312 mm w.e..

The increase of *T* led to reduction of the ratio of snow accumulation to total *P*. Table 2 shows the decadal glacier-wide ratio of snow accumulation to total precipitation, which varied from 0.98 during 1961–1970 to 0.85 during 2001–2010. Generally, the MB of maritime glaciers is less sensitive than that of continental glaciers to variation of *P*. One reason for this is the smaller ratio of snow accumulation to total *P* for maritime

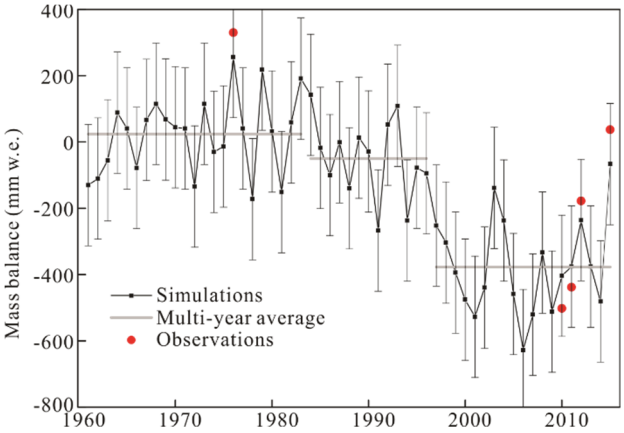

Figure 6. Reconstruction of glacier-wide mass balance during 1960–2015 of the Laohugou Glacier No. 12. Gray lines represent the average mass balance during 1960–1983, 1984–1996, and 1997–2015. Red dots are measured glacier-wide mass balance.

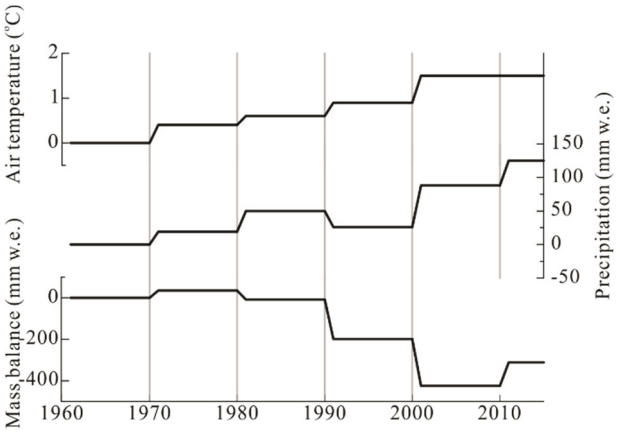

Figure 7. Decadal variations of air temperature, precipitation, and mass balance compared with the average during 1961–1970.

glaciers compared with continental glaciers. For instance, the MB of the Parlung No. 94 Glacier which was a maritime glacier on the southeastern TP was found approximately two to three times more sensitive to a change in T of 1 °C than to 30% variation in P (Yang et al., 2013). However, for the LHG Glacier, a 30% increase in total P during 2010–2011 could approximately offset the change in MB attributable to an increase in T of 1.5 °C (Chen et al., 2017). Zhu et al. (2017) compared MB sensitivities to T and P in relation to the Parlung No. 4 (southeastern TP), Zhadang (southern TP), and Muztag Ata No. 15 (eastern Pamir) glaciers. Their results showed higher MB sensitivity to T by the Parlung No. 4 and the Zhadang glaciers, and higher MB sensitivity to P by the Muztag Ata No. 15 Glacier. It was considered that the most important factor determining the different sensitivities of glacier MB to change in T was the difference in the ratio of snowfall to total P.

5.2 Potential Effect on Mass Balance Caused by Black Carbon

LAPs in snow and ice could accelerate glacier melt. Based on sampling of snow and ice in combination with the use of an energy and mass balance model, Li et al. (2016) indicated that BC could account for 37% of summer melt on the LHG Glacier. Sun et al. (2017) found that the existence of LAPs in surface ice could cause an increase in net shortwave radiation of 7.1–16.0 $W \cdot m^{-2}$ in the ablation zone during June–September, which could result in glacier melt of 1 101–2 663 mm w.e.. Research on lake sediment cores (Han et al., 2015) and ice cores (Wang et al., 2015) has indicated that the amount of BC in northern China has more than doubled since the 1980s (Fig. 8). The DDF is a mathematical expression that reflects the conditions of the glacial surface and of the atmosphere, and BC is one factor that influences the glacial surface condition. Considering such a substantial increase of BC concentration in the snow and ice since the 1980s, it is important to determine whether the MB before 1980s was negatively overestimated when the DDF was calibrated after the 1980s, or whether the MB after the 1980s was negatively underestimated when the DDF was calibrated by measurements before the 1980s.

Figure 8 shows a comparison between simulated MB on the LHG Glacier and measured MB on the Qiyi Glacier and the Urumqi Glacier No. 1. The MBs of the LHG and Qiyi glaciers correspond very well because the two glaciers are separated by only a short distance and they have similar climatic setting. The three glaciers all have experienced intense mass loss since the 1980s, but the magnitude of the losses has varied. The straight lines in Fig. 8 represent the average MBs before and after 1983. It can be seen that the difference in MB of the LHG Glacier before and after 1983 was much less than that of either the Qiyi Glacier or the Urumqi Glacier No. 1. It is demonstrably improper to attribute it to increased BC after the 1980s because the responses of glacier MB to climate change which are influenced by many factors such as the ratio of snowfall to total P, differences in melt energy, and seasonal distribution of P, they varied between the different glaciers (Zhu et al., 2017).

We search glaciers with long-term field MB observations and corresponding simulations. Table 3 presents information regarding three such glaciers. The Golubina glacier in western Tianshan is included in this glacier list in addition to the Qiyi Glacier and the Urumqi Glacier No. 1. Figure 9 shows since the beginning of the 1980s, the TP has experienced overall warming and moistening of the surface air, solar dimming, wind stilling, and more frequent occurrence of deep cloud (Yang et al., 2014). Chen et al. (2018) indicated that increased cloud could cause a decrease of net radiation direct to the glacier surface. Although higher humidity and lower wind speed could depress the energy output of the latent heat flux from the surface, latent heat is comparatively insignificant relative to radiation in relation to glacier melting (Sun et al., 2014, 2012). Therefore, we could rule out the possibility of other meteorological variables leading to the smaller difference.

To quantify intensification of glacier melt caused by the increase of BC after 1980s, we simulated MB of the Urumqi Glacier No. 1 (Fig. 10). The inputs of monthly air temperature and precipitation were from the Daxigou meteorological station with a distance of 2.5 km from the terminus of the glacier, and the data of measured MB was from Dong et al. (2013). The DDF was calibrated by measured MB between 1961–1983 with a constant value of 6.2 $mm \cdot d^{-1} \cdot °C^{-1}$.

Table 2 Decadal average glacier-wide ratio of snow accumulation to total precipitation

Period	Ratio
1961–1970	0.98
1971–1980	0.96
1981–1990	0.94
1991–2000	0.90
2001–2010	0.85
2011–2015	0.86

Table 3 Information of glaciers with long-term field mass balance observations and sources of related mass balance simulations

Glacier name	Latitude (N)	Longitude (E)	Location	Source
Qiyi	39°14′	97°45′	Qilian Mountains	Wang et al. (2017)
Urumqi Glacier No. 1	43°07′	86°49′	Tianshan Mountains	Liu et al. (2015)
Golubina	42°27′	74°30′		Liu et al. (2015)

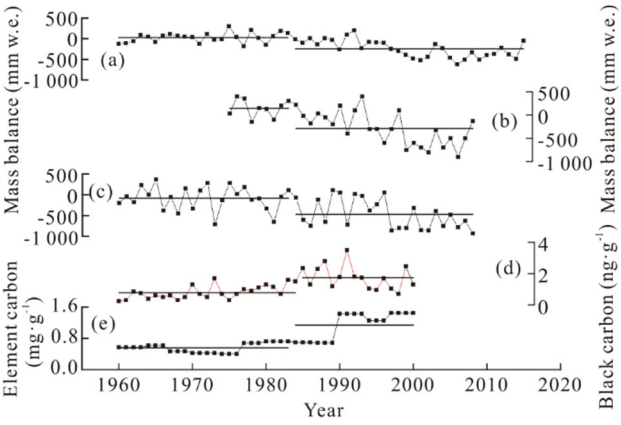

Figure 8. (a) Reconstructed mass balance of Laohugou Glacier No. 12, and measured mass balance of (b) the Qiyi Glacier and (c) the Urumqi Glacier No. 1; (d) black carbon concentration from an ice core located in eastern Pamir (Wang et al., 2015); (e) elemental carbon concentration from sediment core of Lake Qinghai. Straight lines show the average value before and after 1983.

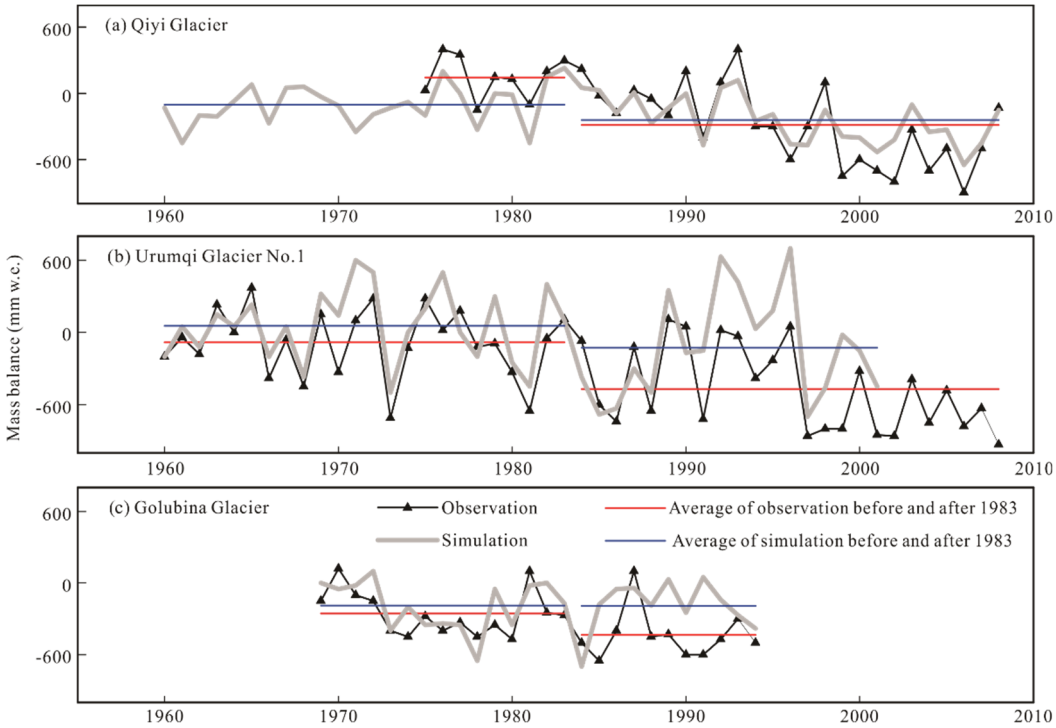

Figure 9. Comparisons between simulated and measured mass balance of (a) the Qiyi Glacier, (b) the Urumqi Glacier No. 1, and (c) the Golubina Glacier. Red straight lines show measured average mass balance before and after 1983. Blue straight lines show simulated average mass balance before and after 1983.

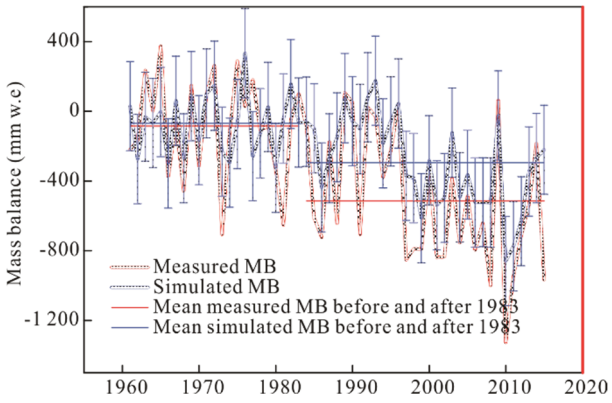

Figure 10. Reconstructed and measured mass balance of Urumqi Glacier No. 1. Red straight lines show measured average mass balance before and after 1983. Blue straight lines show simulated average mass balance before and after 1983.

The total RMSE was 256 mm w.e. between simulation and measurement, and the simulated MB well matched the measured MB during 1961–1983. The mean measured MB was more negative by 220 mm w.e. than simulated MB during 1984–2015, which was equivalent to 26% of glacier ablation (mass balance+ snow accumulation).

The surface albedo of TP glaciers derived from remote sensing imagery has exhibited a decreasing trend during 2001–2011 (Qu et al., 2014; Ming et al., 2012), which could partly be explained by the increase of LAPs (Qu et al., 2014; Ming et al., 2012). Cui et al. (2013, 2010) reported an increasing trend of DDF after the 1980s and they attributed it to surface darkening. Given such a dramatic increase of BC since the 1980s and the well-known influence on glacier melt, we assume that the warming has mainly contributed to the intense glacier melt since the 1980s, but it has been aggravated by the increase of BC in snow and ice.

6 CONCLUSIONS

This study presented a reconstruction of MB during 1961–2015 for the LHG Glacier in the western Qilian Mountains using a temperature-index model. The parameters used in the model were calibrated by measurements of MB and meteorological variables performed on the glacier. The values of T and P were interpolated from measurements recorded at six surrounding national meteorological stations. The calibrated DDF were taken as 7.5 and 3.4 $mm \cdot d^{-1} \cdot °C^{-1}$ for ice and snow, respectively.

Using calibrated parameters, we modeled the MB from 1961–2015. Three periods with different melting rates were roughly identified. During Period I (1961–1984), the glacier-wide MB values were slightly positive with an average MB of 24±276 mm w.e.. During Period II (1984–1995), the MB values became slightly negative with an average MB of -50±276 mm w.e.. The most negative MB values were found during Period III (1996–2015), with an average MB of -377±276 mm w.e.. Climatic analysis indicated that continuous warming contributed most to the increase of glacier mass loss.

Since the 1980s, the amount of BC in northern China has increased considerably. All MB reconstructions in previous studies have shown smaller differences between the average simulated MB than were observed before and after 1984. Meteorological variables that might have influenced the surface energy budget of the glaciers all showed no discernible change before and after the 1980s. Therefore, we concluded that the increase of BC after 1984 increased the DDF and aggravated the glacier mass loss attributable to warming.

ACKNOWLEDGMENTS

The work were supported by the Chinese Academy of Sciences (No. QYZDJ-SSW-DQC039), the National Natural Science Foundation of China (Nos. 41630754, 41721091), the Science and Technology planning Project of Gansu Province (No. 18JR4RA002), and the Project of the State Key Laboratory of Cryospheric Sciences (Nos. SKLCS-OP-2018-06, SKLCS-OP-2019-01), the Open Foundation of State Key Laboratory of Hydrology-Water Resources and Hydraulic Engineering (No. 2017490711). Many thanks are also extended to colleagues working at Qilian Shan Station of Glaciology and Ecological Environment. The final publication is available at Springer via https://doi.org/10.1007/s12583-019-1238-5.

REFERENCES CITED

Azam, M. F., Wagnon, P., Vincent, C., et al., 2014. Reconstruction of the Annual Mass Balance of Chhota Shigri Glacier, Western Himalaya, India, since 1969. *Annals of Glaciology*, 55(66): 69–80. https://doi.org/10.3189/2014aog66a104

Bond, T. C., Streets, D. G., Yarber, K. F., et al., 2004. A Technology-Based Global Inventory of Black and Organic Carbon Emissions from Combustion. *Journal of Geophysical Research*, 109: D14203. https://doi.org/10.1029/2003jd003697

Che, Y. J., Zhang, M. J., Li, Z. Q., et al., 2017. Glacier Mass-Balance and Length Variation Observed in China during the Periods 1959–2015 and 1930–2014. *Quaternary International*, 454: 68–84. https://doi.org/10.1016/j.quaint.2017.07.003

Chen, J., Kang, S., Qin, X., et al., 2017. The Mass-Balance Characteristics and Sensitivities to Climate Variables of Laohugou Glacier No. 12, Western Qilian Mountains, China. *Science in Cold and Arid Regions*, 9(6): 543–553. https://doi.org/10.3724/sp.j.1226.2017.00543

Chen, J. Z., Qin, X., Kang, S. C., et al., 2018. Effects of Clouds on Surface Melting of Laohugou Glacier No. 12, Western Qilian Mountains, China. *Journal of Glaciology*, 64(243): 89–99. https://doi.org/10.1017/jog.2017.82

Cui, Y. H., Ye, B. S., Wang, J., et al., 2010. Analysis of the Spatial-Temporal Variations of the Positive Degree-Day Factors on the Glaicer No. 1 at the Headwaters of the Urumqi River. *Journal of Glaciology and Geocryology*, 32(2): 265–274 (in Chinese with English Abstract)

Cui, Y. H., Ye, B. S., Wang, J., et al., 2013. Influence of Degree-Day Factor Variation on the Mass Balance of Glacier No. 1 at the Headwaters of Urumqi River, China. *Journal of Earth Science*, 24(6): 1008–1022. https://doi.org/10.1007/s12583-013-0394-2

Dong, Z. W., Qin, D. H., Ren, J. W., et al., 2013. The Response of Equilibrium Line Altitude to Climate Change in the Past 50 Years on the Urumqi Glacier No. 1. *Chinese Science Bulletin*, 58(9): 825–832 (in Chinese with English Abstract)

Dong, Z. W., Qin, D. H., Kang, S. C., et al., 2016. Individual Particles of Cryoconite Deposited on the Mountain Glaciers of the Tibetan Plateau: Insights into Chemical Composition and Sources. *Atmospheric Environment*, 138: 114–124. https://doi.org/ 10.1016/j.atmosenv.2016.05.020.

Dong, Z. W., Shao, Y. P., Qin, D. H., et al., 2018a. Insight into Radio-Isotope 129I Deposition in Fresh Snow at a Remote Glacier Basin of Northeast Tibetan Plateau, China. *Geophysical Research Letters*, 45(13): 6726–6733. https://doi.org/10.1029/2018gl078480

Dong, Z. W., Kang, S. C., Qin, D. H., et al., 2018b. Variability in Individual Particle Structure and Mixing States between the Glacier-Snowpack and Atmosphere in the Northeastern Tibetan Plateau. *The Cryosphere*, 12(12): 3877–3890. https://doi.org/10.5194/tc-12-3877-2018

Dong, Z. W., Qin, D. H., Li, K. M., et al., 2019. Spatial Variability, Mixing States and Composition of Various Haze Particles in Atmosphere during Winter and Summertime in Northwest China. *Environmental Pollution*, 246: 79–88. https://doi.org/ 10.1016/j.envpol.2018.11.101

Du, W. T., Qin, X., Sun W. J., et al., 2011. Reconstruction of Air Temperature at Glacier Area in Mountain—A Case of Laohugou Glacier Area. *Journal of Arid Land Resources Environment*, 25: 149–154 (in Chinese with English Abstract)

Flanner, M. G., Zender, C. S., Randerson, J. T., et al., 2007. Present-Day Climate Forcing and Response from Black Carbon in Snow. *Journal of Geophysical Research*, 112: D11202. https://doi.org/10.1029/2006jd008003

Fujita, K., Ageta, Y., 2000. Effect of Summer Accumulation on Glacier Mass Balance on the Tibetan Plateau Revealed by Mass-Balance Model. *Journal of Glaciology*, 46(153): 244–252. https://doi.org/10.3189/172756500781832945

Gardelle, J., Berthier, E., Arnaud, Y., 2012. Slight Mass Gain of Karakoram Glaciers in the Early Twenty-First Century. *Nature Geoscience*, 5(5): 322–325. https://doi.org/10.1038/ngeo1450

Gardelle, J., Berthier, E., Arnaud, Y., et al., 2013. Region-Wide Glacier Mass Balances over the Pamir-Karakoram-Himalaya during 1999–2011. *The Cryosphere*, 7(4): 1263–1286. https://doi.org/10.5194/tc-7-1263-2013

Guo, W. Q., Liu, S. Y., Xu, J. L., et al., 2015. The Second Chinese Glacier Inventory: Data, Methods and Results. *Journal of Glaciology*, 61(226): 357–372. https://doi.org/10.3189/2015jog14j209

Han, Y. M., Wei, C., Bandowe, B., et al., 2015. Elemental Carbon and Polycyclic Aromatic Compounds in a 150-Year Sediment Core from Lake Qinghai, Tibetan Plateau, China: Influence of Regional and Local Sources and Transport Pathways. *Environmental Science & Technology*, 49(7): 4176–4183. https://doi.org/10.13039/501100001711

Hock, R., 2003. Temperature Index Melt Modelling in Mountain Areas. *Journal of Hydrology*, 282(1–4): 104–115. https://doi.org/10.1016/s0022-1694(03)00257-9

Hock, R., Holmgren, B., 2005. A Distributed Surface Energy-Balance Model for Complex Topography and Its Application to Storglaciären, Sweden. *Journal of Glaciology*, 51(172): 25–36. https://doi.org/10.3189/172756505781829566

Huss, M., Farinotti, D., Bauder, A., et al., 2008. Modelling Runoff from Highly Glacierized Alpine Drainage Basins in a Changing Climate. *Hydrological Processes*, 22(19): 3888–3902. https://doi.org/10.1002/hyp.7055

Immerzeel, W. W., van Beek, L. P. H., Bierkens, M. F. P., 2010. Climate Change will Affect the Asian Water Towers. *Science*, 328(5984): 1382–1385. https://doi.org/10.1126/science.1183188

IPCC. 2013. Climate Change 2013: The Physical Science Basis. Contribution of Working Group I to the Fifth Assessment Report of the Intergovernmental Panel on Climate Change. Cambridge University Press, Cambridg

Kang, S. C., Xu, Y. W., You, Q. L., et al., 2010. Review of Climate and Cryospheric Change in the Tibetan Plateau. *Environmental Research Letters*, 5(1): 015101. https://doi.org/10.1088/1748-9326/5/1/015101

Kayastha, R. B., Ageta, Y., Nakawo, M., et al., 2003. Positive Degree-Day Factors for Ice Ablation on Four Glaciers in the Nepalese Himalayas and Qinghai-Tibetan Plateau. *Bulletin of Glaciological Research*, 20: 7–14

Kopacz, M., Mauzerall, D. L., Wang, J., et al., 2011. Origin and Radiative Forcing of Black Carbon Transported to the Himalayas and Tibetan Plateau. *Atmospheric Chemistry and Physics*, 11(6): 2837–2852. https://doi.org/10.5194/acp-11-2837-2011

Kraaijenbrink, P. D. A., Bierkens, M. F. P., Lutz, A. F., et al., 2017. Impact

of a Global Temperature Rise of 1.5 Degrees Celsius on Asia's Glaciers. *Nature*, 549(7671): 257–260. https://doi.org/10.1038/nature23878

Li, Y., Chen, J. Z., Kang, S. C., et al., 2016. Impacts of Black Carbon and Mineral Dust on Radiative Forcing and Glacier Melting during Summer in the Qilian Mountains, Northeastern Tibetan Plateau. *The Cryosphere Discussions*, 1–14. https://doi.org/10.5194/tc-2016-32

Li, Z. Q., Li, H. L., Chen, Y. N., 2011. Mechanisms and Simulation of Accelerated Shrinkage of Continental Glaciers: A Case Study of Urumqi Glacier No. 1 in Eastern Tianshan, Central Asia. *Journal of Earth Science*, 22(4): 423–430. https://doi.org/10.1007/s12583-011-0194-5

Liu, Q., Liu, S. Y., 2015. Response of Glacier Mass Balance to Climate Change in the Tianshan Mountains during the Second Half of the Twentieth Century. *Climate Dynamics*, 46(1/2): 303–316. https://doi.org/10.1007/s00382-015-2585-2

Liu, S. Y., Sun, W. X., Shen, Y. P., et al., 2003. Glacier Changes since the Little Ice Age Maximum in the Western Qilian Shan, Northwest China, and Consequences of Glacier Runoff for Water Supply. *Journal of Glaciology*, 49(164): 117–124. https://doi.org/10.3189/172756503781830926

Liu, Y. S., Qin, X., Chen, J. Z., et al., 2018. Variations of Laohugou Glacier No. 12 in the Western Qilian Mountains, China, from 1957 to 2015. *Journal of Mountain Science*, 15(1): 25–32. https://doi.org/10.1007/s11629-017-4492-y

Lutz, A. F., Immerzeel, W. W., Shrestha, A. B., et al., 2014. Consistent Increase in High Asia's Runoff Due to Increasing Glacier Melt and Precipitation. *Nature Climate Change*, 4(7): 587–592. https://doi.org/10.1038/nclimate2237

Mölg, T., Cullen, N. J., Hardy, D. R., et al., 2009. Quantifying Climate Change in the Tropical Midtroposphere over East Africa from Glacier Shrinkage on Kilimanjaro. *Journal of Climate*, 22(15): 4162–4181. https://doi.org/10.1175/2009jcli2954.1

Marzeion, B., Cogley, J. G., Richter, K., et al., 2014. Attribution of Global Glacier Mass Loss to Anthropogenic and Natural Causes. *Science*, 345(6199): 919–921. https://doi.org/10.1126/science.1254702

Maussion, F., Scherer, D., Mölg, T., et al., 2014. Precipitation Seasonality and Variability over the Tibetan Plateau as Resolved by the High Asia Reanalysis. *Journal of Climate*, 27(5): 1910–1927. https://doi.org/10.1175/jcli-d-13-00282.1

Ming, J., Du, Z. C., Xiao, C. D., et al., 2012. Darkening of the Mid-Himalaya Glaciers since 2000 and the Potential Causes. *Environmental Research Letters*, 7(1): 014021. https://doi.org/10.1088/1748-9326/7/1/014021

Morrill, C., Overpeck, J. T., Cole, J. E., 2003. A Synthesis of Abrupt Changes in the Asian Summer Monsoon since the Last Deglaciation. *The Holocene*, 13(4): 465–476. https://doi.org/10.1191/0959683603hl639ft

Qian, Y., Flanner, M. G., Leung, L. R., et al., 2011. Sensitivity Studies on the Impacts of Tibetan Plateau Snowpack Pollution on the Asian Hydrological Cycle and Monsoon Climate. *Atmospheric Chemistry and Physics*, 11(5): 1929–1948. https://doi.org/10.5194/acp-11-1929-2011

Qu, B., Ming, J., Kang, S. C., et al., 2014. The Decreasing Albedo of the Zhadang Glacier on Western Nyainqentanglha and the Role of Light-Absorbing Impurities. *Atmospheric Chemistry and Physics*, 14(20): 11117–11128. https://doi.org/10.5194/acp-14-11117-2014.

Scherler, D., Bookhagen, B., Strecker, M. R., 2011. Spatially Variable Response of Himalayan Glaciers to Climate Change Affected by Debris Cover. *Nature Geoscience*, 4(3): 156–159. https://doi.org/10.1038/ngeo1068

Sun, W. J., Qin, X., Du, W. T., et al., 2014. Ablation Modeling and Surface Energy Budget in the Ablation Zone of Laohugou Glacier No. 12, Western Qilian Mountains, China. *Annals of Glaciology*, 55(66): 111–120. https://doi.org/10.3189/2014aog66a902

Sun, W. J., Qin, X., Ren, J. W., et al., 2012. The Surface Energy Budget in the Accumulation Zone of the Laohugou Glacier No. 12 in the Western Qilian Mountains, China, in Summer 2009. *Arctic*, *Antarctic*, *and Alpine Research*, 44(3): 296–305. https://doi.org/10.1657/1938-4246-44.3.296

Sun, W. J., Qin, X., Wang, Y. T., et al., 2017. The Response of Surface Mass and Energy Balance of a Continental Glacier to Climate Variability, Western Qilian Mountains, China. *Climate Dynamics*, 50(9/10): 3557–3570. https://doi.org/10.1007/s00382-017-3823-6.

Sun, Z., Xie, Z., 1981. Recent Variation and Trend of the Laohugou Glacier No. 12, Qilian Mountains. *Chinese Science Bulletin*, 26(6): 366–369 (in Chinese with English Abstract)

Tian, H. Z., Yang, T. B., Liu, Q. P., 2014. Climate Change and Glacier Area Shrinkage in the Qilian Mountains, China, from 1956 to 2010. *Annals of Glaciology*, 55(66): 187–197. https://doi.org/10.3189/2014aog66a045

Wang, M., Xu, B. Q., Kaspari, S. D., et al., 2015. Century-Long Record of Black Carbon in an Ice Core from the Eastern Pamirs: Estimated Contributions from Biomass Burning. *Atmospheric Environment*, 115: 79–88. https://doi.org/10.1016/j.atmosenv.2015.05.034.

Wang, B., 2004. A Study on Synthetic Differentiation Method for Basic Meteoro-Logical Data Quality Control. *Journal of Applied Meteorology Science*, 15: 51–59

Wang, N. L., He, J. Q., Pu, J. C., et al., 2010. Variations in Equilibrium Line Altitude of the Qiyi Glacier, Qilian Mountains, over the Past 50 Years. *Chinese Science Bulletin*, 55(33): 3810–3817. https://doi.org/10.1007/s11434-010-4167-3

Wang, S., Yao, T. D., Tian, L. D., et al., 2017. Glacier Mass Variation and Its Effect on Surface Runoff in the Beida River Catchment during 1957–2013. *Journal of Glaciology*, 63(239): 523–534. https://doi.org/10.1017/jog.2017.13

Xu, B. Q., Cao, J. J., Hansen, J., et al., 2009. Black Soot and the Survival of Tibetan Glaciers. *Proceedings of the National Academy of Sciences*, 106(52): 22114–22118. https://doi.org/10.1073/pnas.0910444106

Xu, M., Han, H., Kang, S., 2017. The Temporal and Spatial Variation of Positive Degree-Day Factors on the Koxkar Glacier over the South Slope of the Tianshan Mountains, China, from 2005 to 2010. *Science in Cold and Arid Regions*, 9(5): 425–431 https://doi.org/10.3724/SP.J.1226.2017.00425

Yang, K., Wu, H., Qin, J., et al., 2014. Recent Climate Changes over the Tibetan Plateau and Their Impacts on Energy and Water Cycle: A Review. *Global and Planetary Change*, 112: 79–91. https://doi.org/10.1016/j.gloplacha.2013.12.001

Yang, W., Yao, T. D., Guo, X. F., et al., 2013. Mass Balance of a Maritime Glacier on the Southeast Tibetan Plateau and Its Climatic Sensitivity. *Journal of Geophysical Research*: *Atmospheres*, 118(17): 9579–9594. https://doi.org/10.1002/jgrd.50760

Yao, T. D., Thompson, L., Yang, W., et al., 2012. Different Glacier Status with Atmospheric Circulations in Tibetan Plateau and Surroundings. *Nature Climate Change*, 2(9): 663–667. https://doi.org/10.1038/nclimate1580

Zhang, Y., Liu, S. Y., Ding, Y. J., 2006. Observed Degree-Day Factors and Their Spatial Variation on Glaciers in Western China. *Annals of Glaciology*, 43: 301–306. https://doi.org/10.3189/172756406781811952

Zhu, M. L., Yao, T. D., Yang, W., et al., 2017. Differences in Mass Balance Behavior for Three Glaciers from Different Climatic Regions on the Tibetan Plateau. *Climate Dynamics*, 50(9/10): 3457–3484. https://doi.org/10.1007/s00382-017-3817-4